AIAA AVIATION Forum
8-12 June 2026, San Diego, CA
AIAA AVIATION 2026 Forum
10.2514/6.2026-4094

Development and Flight Testing of the Bronco UAV Testbed for Airborne Event-Based Sensing: Part 1

Paul Coen* Brendan Cox† and Or D. Dantsker‡
Indiana University, Bloomington, IN 47408

Event cameras are a promising sensing modality for aviation systems because they provide asynchronous microsecond-scale measurements and high dynamic range in challenging lighting environments. Despite growing interest in event-based perception for mobile robotics, existing flight datasets and demonstrations remain limited for long-endurance fixed-wing aircraft. This paper presents the preliminary development of a fixed-wing unmanned aircraft system intended to support a large multimodal sensor payload for future stereo event-camera dataset collection. The planned payload includes two Triton2 EVS event cameras, four synchronized global-shutter frame cameras, inertial sensing, onboard computation, data acquisition hardware, and independent payload power. Initial bench top testing was used to estimate the system-level compute, bandwidth, and mass requirements, resulting in a target instrumentation payload of approximately 4.28 kg. These requirements were used to define aircraft selection criteria based on payload capacity, internal volume, vibration mitigation, endurance, flight speed range, and regulatory weight limits. A commercial radio-control aircraft trade study was conducted, and the Hangar 9 OV-10 Bronco 30cc ARF was selected as the development testbed due to its twin-engine configuration, available payload volume, and compatibility with the 55 lb operating constraint. The aircraft was modified to improve reliability, reduce nonessential mass, and support future payload integration efforts. An initial baseline flight test was conducted in the stock-weight configuration to verify aircraft assembly, control response, propulsion-system operation, flap functionality, and general handling qualities before payload integration. The aircraft successfully completed takeoff, climb, racetrack-pattern flight, approach, and touchdown; however, a partial landing-gear failure occurred during the rollout when the left wheel separated from the axle due to loss of the retaining C-clip. This issue prevented additional flights and deferred the planned evaluation of alternate propulsion and payload configurations to future work. Despite this limitation, the initial flight demonstrated the viability of the selected aircraft platform and identified key reliability improvements required before full payload testing. This work establishes the aircraft, integration approach, and flight-test methodology needed for future collection of fixed-wing stereo event-camera data and subsequent evaluation of event-based perception algorithms in realistic aviation environments.

Nomenclature

ESC	=	Electronic Speed Controller
FoV	=	Field of View
GNSS	=	Global Navigation Satellite System
HMI	=	Human Machine Interface
IMU	=	Inertial Measurement Unit
MP	=	Megapixel
PoE	=	Power over Ethernet
RC	=	Radio Control
SWAP	=	Size, Weight, and Power
UART	=	Universal Asynchronous Receiver/Transmitter
UAV	=	Uncrewed Aerial Vehicle
USB	=	Universal Serial Bus

*PhD Student, Department of Computer Science. pcoen@iu.edu. Scientist, Naval Surface Warfare Center Crane Division. AIAA Student Member.
†PhD Student, Department of Intelligent Systems Engineering. brewcox@iu.edu. AIAA Student Member.
‡Assistant Professor, Department of Intelligent Systems Engineering, odantske@iu.edu. AIAA Member.

I. Introduction

Subscale flight testing enables rapid evaluation of new sensor systems in realistic aviation scenarios. Event cameras represent a new modality of vision systems that are based around biological vision. They are able to capture changes in irradiance at microsecond timescales asynchronously across different pixels. The new variety of sensor also has an extremely high dynamic range compared to traditional frame-based sensors. This makes them well suited to aviation problems that require high-speed decision-making across high dynamic range environments.

Additional work has been done to apply these sensors to mobile robotic applications such as autonomous driving [1] and multi-rotor UAV systems [2–6] in which fast decision-making is needed. Additional work has been done to estimate the position of an ego vehicle as well as work to identify and track external objects using event cameras .[7–24] Although these domains present new challenges to test various algorithms, they fail to address long-endurance fixed-wing flight applications. Recent work has addressed the initial integration needed to fly and test these sensors on-board using an existing unmanned aircraft.[25] The initial work on this was limited in scope and application though as its focus was on identifying the viability of these sensors for common aviation specific problems.

To address these concerns, a new large-scale event camera dataset is needed to complement current datasets with data from fixed-wing flight systems. To collect this, a new sensor payload is needed to support fixed-wing aircraft specific problem such as object avoidance at high speeds. This work takes the first step towards this by designing a new UAS with an ideal sensor payload that is over 10lbs. This work discusses the sensor payload required for the UAS, however the focus of this work is on flight testing required for development of the new UAS in support of these payload requirements.

The design of the new sensor suite and data collection system is planned to overcome the limitations of the previous single-camera platform in a multitude of ways. Depth information is needed to estimate the distance of objects from moving robotic platforms. Prior work has explore using event cameras in stereo configurations using datasets such as MVSEC[26] and DSEC.[27] Event cameras provide data with high temporal resolution at a microsecond level and high dynamic range. This makes them well suited for when flying in dynamic lighting conditions. Frame cameras provide full-view texture-rich, synchronous images that serve as a conventional baseline and ground truth for comparative analysis to objects in the environment.

Figure 1. Flight-ready Hangar 9 OV-10 Bronco 30cc UAV testbed prepared for initial flight evaluation. The aircraft was configured with the stock electric twin-engine configuration and prepared without the full sensor payload installed.

The remainder of this work is organized in the following order: Section II builds out the needed requirements for a large fixed-wing UAS to support the new large multi-sensor suite. Section III delineates the process taken to build the aircraft and details the preliminary weight breakdown of the sensor payload. Section IV discusses and reports the flight testing performed with the new UAS to support a larger payload capacity. Additionally, optimizations taken to reduce weight and improve flight performance are discussed. Section V then summarizes this papers discoveries and results. Lastly, Section VI outlines the future work planned for this UAS.

II. Preliminary Development of Sensor Suite and Data Collection System

The goal of this work is to enable the capture of the first meaningful fixed-wing stereo event camera dataset. The system architecture consists of two sensor clusters on each side of the aircraft. Both with the same sensor payloads connected to a central data collection system on the aircraft. A stereo pair of event cameras and two stereo pairs of conventional global shutter frame cameras will be used. The frame cameras in each sensor cluster will each have one RGB camera and one grayscale camera to compare the differing sensitivities of both types of sensors to event-based data. This multi-stereo design is needed for depth sensitive designs to ensure the cameras have similar baselines across the desired system.

The event cameras used will be the same Triton 2 EVS 0.9MP as prior work as these give the highest resolution sensor with a secure mounting system. Two will be used to support stereo vision applications. They will be powered by two PoE injectors connected to the distinct ports on the back of the MSI Cubi computer from the initial bench top test detailed later. The lens used for each will be a telescopic varifocal lens with focal lengths ranging from 5mm to 50mm to enable additional stereo test setups with differing focal lengths. This will enable differing zoom levels using both cameras in a different test configuration. An example of this alternative configuration is given in Fig. 5 that shows the 4mm lens used from prior work[25] to the new varifocal lens in this work in the 5mm configuration.

Although the primary focus of the new sensor system is to test and validate new algorithms developed for event-based sensing on aviation platforms, it will also support more commonly used frame cameras to compare against prior work. The RGB cameras capture full-color video at 1920x1200 with a 82deg HFoV[28] while the grayscale cameras capture at 1280x800 with a 80deg HFoV.[29] These are all synchronized with and recorded on an OAK-FFC 4P board.[30] This reduces computation needs for the primary computation node and allows for 20fps data recording which will be needed for comparison to other hybrid event camera/frame camera datasets such as MVSEC[26] and DSEC.[27] An example of this frame data from a bench top test is given in Fig. 3(a).

RGB sensors typically have lower light sensitivity due to their Bayer filter as can be seen by comparing both camera chipset data sheets. The grayscale camera has been included to account for this reduced sensitivity of the RGB sensor. The grayscale sensors should be better suited for low-light conditions to compare against the event camera and gives

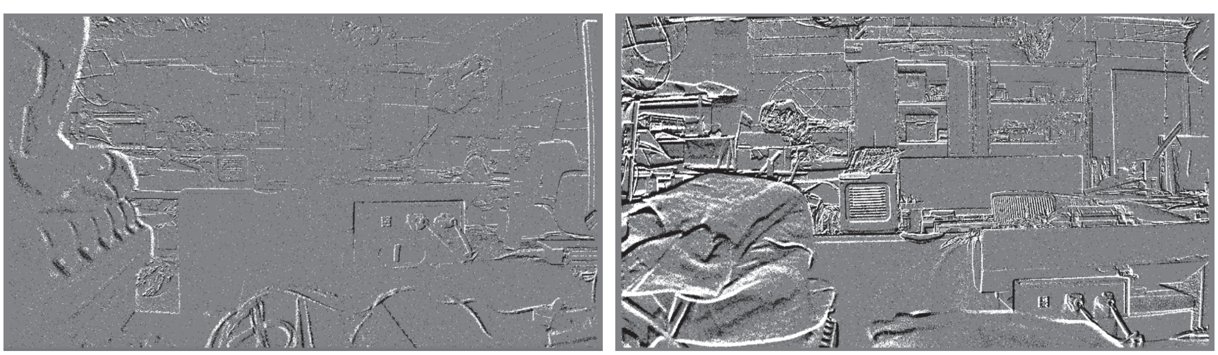

(a) (b)

Figure 2. A 33ms event integration of the 4mm focal length lens on one of two event cameras is picture in (a). The second event camera with a 5mm focal length lens showing the same integration is given in (b). The picture shows the experiment used to determine which lens will be selected for the full aircraft. The camera in (b) is slightly behind the camera pictured in (a).

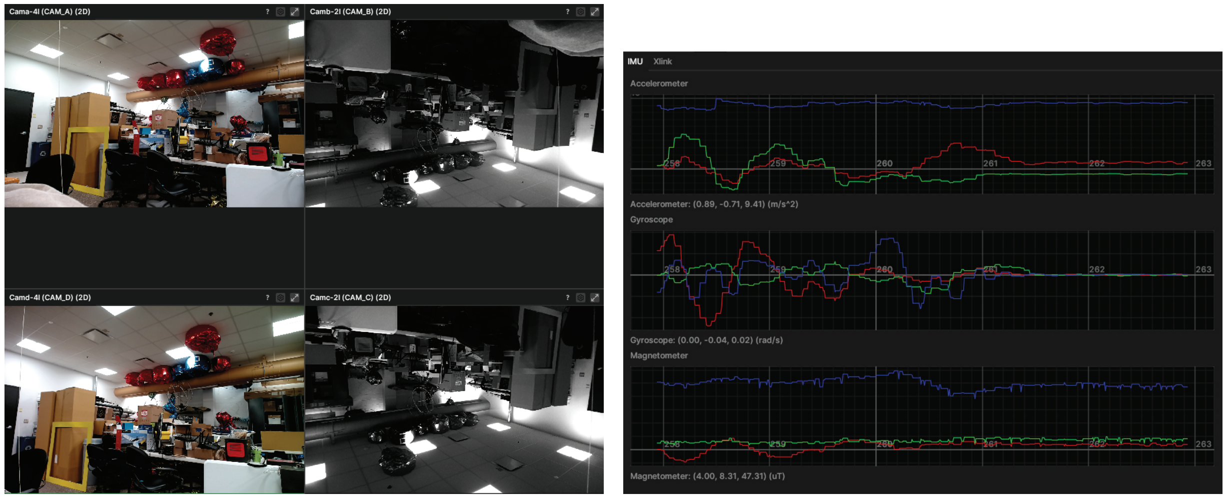

(a) (b)

Figure 3. Frames from each of the four cameras included in the improved frame camera system are given in (a). The grayscale frames are flipped due to mounting position and will be flipped in software in the future implementation. Redundant IMU data from the frame-camera collection system is also displayed in (b) during the same period as the images.

a direct comparison for validating event-based frame reconstruction algorithms such as E2VID,[31] which generate grayscale video output from the event data stream.

Autonomous navigation of a fixed-wing UAV requires of high-fidelity 6DOF localization and navigation system. This sensor allows for representation of the aircraft's relative position and orientation from the ground. The newly developed UAV will utilize an identical IMU from the last system, however it will utilize the full data rate due to the new computation available with a better computer. This takes the IMU data rate from the 100Hz seen in prior work[25] to 1000Hz. This higher rate should allow for better localization estimation. An additional 100Hz IMU included with the the camera controller is pictured in Fig. 3(b) that will be used to reduce error from both IMU systems through the use of Kalman filtering.

A bench top setup was made using the equipment listed in Table 2 to evaluate an early version of the new data collection system. Data from this setup can be seen in Fig. 5 and in Fig. 3. The event cameras when both were recording to disk and used approximately 45% CPU utilization while the four frame cameras at 20fps utilized 30% CPU utilization. Both sensor tests exhibited spikes in this usage, however frame cameras will be recorded to the SD card available on the OAK-FFC 4P board which will reduce overall actual CPU usage. This early test gives a good indication that the data collection system will have sufficient computation spare for vision-based downstream tasks and eventual autonomy applications.

The move to a multi-modal dual sensor system created a new set of interdependent hardware requirements. Based on the initial bench top test, the simultaneous operation of two event cameras and four frame cameras in addition to a 100Hz IMU, generates quite a large bandwidth data stream. This stream greatly exceeds the processing ability of the previous computer used. This necessitated the use of a new computer system with additional compute cores with higher clock speeds. The new computer used differs in that it uses a 19.5V interface instead of the original 12V from the initial paper. It also consumes more power on average, going up to 120W at worst. This consumption in addition to the six cameras and other peripherals like the two PoEs require a complete redesign of the data collection power system. Two high-capacity 6S batteries will be used for the new system to provide power for approximately 30 to 45 minutes of flight time.

III. Aircraft Requirements

The bench top setup in Table 2 was used as the target payload weight needed for the final UAV design. To select an aircraft suitable for testing the data recording payload, relevant legal requirements for flying UAVs in the USA were first considered. To minimize licensing dependencies for the new aircraft, the university was able to operate under non–FAA

Table 1. Sensor system weights and specifications.

Component	Description	Weight (grams)
Autonomy Hardware		
Computer		
Computer	MSI Cubi NUC 1MG-007US Intel Core 7 150U	667
Camera Control System	OAK-FFC 4P with Mounting Frame	261
Sensors		
Event Cameras	(2) Triton2 EVS 0.9 MP Model (IMX636)	234
Event Camera Lens	(2) Zowietek 5-50mm 12MP C-Mount Low Distortion Zoom Lens	208
Global Shutter RGB Camera	(2) OAK-FFC AR0234 (lens incl.)	18
Global Shutter Grayscale Camera	(2) OAK-FFC OV9282 (lens incl.)	6
Power		
Battery	(2) Thunder Power Elite 25c 6S 22.2V 5000 mAh	1,390
Interface		
PoE Switch	(2) Industrial 2.5 Gigabit PoE+ Injector with 12-48V DC Input	112
Cables	Power cables and data cables	450
Camera Mounting Frame	4ft 20x20mm T-Slotted Aluminum Frame Rail	553
Flight Control and Data Acquisiton System		
Computer		
Flight system	Al Volo FC+DAQ 400 Hz system	150
Sensors		
Inertial Measurement Unit	Xsens IMU GNSS/INS MTI-G-710 Series	58
Airspeed sensor	Al Volo Pitot Static Airspeed Sensor	4
Motor sensor	(2) Al Volo Castle ESC Interface	12
Power		
Regulator	Built into FC+DAQ	0 (incl.)
Battery	Thunder Power ProLiteX 3S 1350 mAh	95
Interface		
Data Downlink	900 MHz serial radio	55
Onboard	UART serial interface	5
Configuration	Wifi-based interface	0 (incl.)
	Total Weight	4,278

Part 107 recreational flight rules, as outlined in U.S.C. Title 49, Section 44809.[32] These rules restrict the total takeoff weight to less than 55 lbs. Accordingly, candidate scale aircraft must be in a target weight range of approximately 30 to 45.5 lbs.

A primary requirement for candidate aircraft was an expansive internal payload capacity. This was necessitated by the substantial volumetric footprint of the bench-top sensor suite. Since the bench-top prototype has not yet undergone SWaP reductions, the selected platform was required to provide surplus internal volume to aid in mounting options. Specifically, the aircraft's internal payload bay needed to accommodate custom structural mounting brackets, permit adequate clearance for cable routing, and allow for the future installation of vibration isolation systems to ensure the operational stability of the payload during flight.

Figure 4. The single frame camera and an event camera used for data collection on the original experimentation UAV.[25]

An additional consideration is mitigation of the vibrational effects caused by the motor seen in initial work on fixed-wing mounted event cameras. The primary issue seen in that work was vibration issues caused by both the mounting system and the vibrational noise introduced by motor. By mounting the camera on a boom mounted to the wing, the initial work caused an exaggerated amount of vibration in all data collected. The vibration in the event data is thought to be caused by the vibration of the motor and exaggerated through the wing mounted boom on the right side of the airframe in Fig. 4. The new platform will mitigate this vibration effect by centrally mounting the cameras in a way to minimize exaggerated noise by aircraft motion. Additionally, it will need to utilize counter rotating propellers on with a twin engine configuration to reduce the impacted by motor vibrational noise. Lastly, the sensor mounts and data capture system will use vibration isolators with all mounting points directly connected to the aircraft Like before, the sensor systems will be mounted forward to the engines to eliminate noisy vibration signal seen in the event data added by propeller motion.

To effectively support future testing of planned autonomy systems, the candidate aircraft must operate within a widely defined flight envelope. The platform is required to maintain stable, controlled flight across a broad velocity range, targeting operational speeds between 9 m/s and 45 m/s. This wide speed profile will enable evaluating the performance and responsiveness of the data collection payload and future onboard autonomous systems under varying dynamic conditions. Furthermore, the aircraft must possess a continuous flight endurance between 10 and 20 minutes. This operational window provides sufficient duration for sustained data acquisition, execution of extended autonomous flight paths, and comprehensive algorithm validation in a single flight, thereby maximizing the efficiency of planned field-testing.

IV. COTS Radio Control Model Comparison

To select an appropriate aircraft given the prior requirements, a trade study was performed to identify available aircraft from various manufacturers at the time of writing. Manufacturers compared against include Bill Hempel, CARF-Models, Extreme Flight, Flex Innovations, Hangar 9, Legacy Aviation, RC Warbird Models, Seagull Models, SebArt, TMMY Composite, and Skymaster Jet Models. A subject-matter expert with 20+ years of RC model airplane experience was consulted to provide suggestions for aircraft to select.

Aircraft were generally selected from propeller-driven scale models of general aviation and military aircraft. Although a few aerobatic examples are included, these aircraft were not the primary focus because they are typically smaller and designed for high-G maneuvering rather than higher payload capacity. Model jets were also excluded because, while optimized for speed, they generally offer very limited payload capability. Overall, the selection emphasized slow- to medium-speed aircraft, such as Cub-style models and other conventional propeller-driven designs, while avoiding very high-speed aircraft such as jets.

Although larger model aircraft above the 55 lb limit have been used successfully in prior flight research, they were not considered suitable for the present work due to the previously discussed operational and regulatory constraints. Examples include large Cub-type airframes such as the Hangar 9 100–200 cc Cub and the 60% Bill Hempel Cub used in NASA's MicroCub project,[33] as well as the TMMY Composite 35% Cessna platform used for distributed electric propulsion research.[34] These aircraft demonstrate that larger RC-scale platforms can provide useful payload and integration capability; however, the present comparison intentionally focuses on aircraft that can remain below 55 lb while still offering sufficient size, payload margin, and geometric flexibility for the intended modifications.

Figure 6 summarizes the trade study by comparing the available weight margin below the 55 lb maximum takeoff weight limit with the percentage increase required from each aircraft's baseline weight. The Hangar 9 OV-10 Bronco 30cc was identified as the first aircraft in the trade space to provide more than 10 lb of available weight capacity while requiring one of the smallest increases in baseline aircraft weight. Specifically, the Bronco 30cc provided approximately 13 lb of additional capacity before reaching the 55 lb limit, making it a favorable balance between payload margin and required aircraft modification. This was important because remaining below 55 lb preserved FAA compliance while still allowing sufficient margin for additional batteries, instrumentation, and experimental hardware. The Bronco 30cc was also attractive because its twin-engine configuration aligned with the design goals discussed in the previous section. In addition, because the aircraft is a scale model with several aesthetic components that do not serve a functional purpose, some weight reduction was expected to be possible, allowing additional mass to be reallocated toward batteries or other mission-critical systems.

Figures 7 and 8 further compare the candidate aircraft by considering wingspan relative to wing loading and cubic wing loading at the 55 lb maximum takeoff weight. These metrics were important because the selected aircraft needed to provide favorable flight characteristics while also remaining practical for transportation, storage, assembly, and field operations. In general, aircraft located toward the lower-left region of these plots were preferred because they combined a smaller wingspan with lower aerodynamic loading. Conventional wing loading provided a direct comparison of aircraft weight relative to wing area, while cubic wing loading provided an additional scale-normalized metric that better accounts for differences in aircraft size. Based on these criteria, the Hangar 9 OV-10 Bronco 30cc and the Flex Innovations RV-8 70cc G2 were among the most favorable candidates. However, although the RV-8 performed well in the span-loading comparison, it required a much larger percentage increase from its baseline flight weight to reach 55 lb, making it less suitable for the intended configuration. Therefore, the Bronco 30cc provided the more practical compromise by combining relatively low loading, manageable wingspan, acceptable weight growth, and the desired twin-engine configuration.

Table 2. Model RC aircraft comparison.

Aircraft	Manufacturer (Distributor)	Wingspan (in.)	Length (in.)	Wing Area (sq. in.)	Baseline Flight Weight (lb)	Weight Available under 55 lb (lb)	Weight Increase to 55 lb (%)	Wing Loading at 55 lb (oz/ft^2)	Cubic Loading at 55 lb (oz/ft^3)	Airframe + Gear + S&H Cost (USD)	Previous research use of aircraft or similar
25% Piper J-3 Clipped Wing Cub[35]	Bill Hempel	90	74*	1,400	15.5	39.5	255	90.5	5.8	$730	-
25% Piper PA-25 Pawnee[36]	Bill Hempel	108	71*	1,575	20	35	175	80.5	5.5	$750	-
40% Piper J-3 Clipped Wing Cub[37]	Bill Hempel	144	118	3,340*	40	15	38	37.9	1.6	$2,050	-
40% Piper PA-18 Super Cub[38]	Bill Hempel	168	118	4,110*	40	15	38	30.8	1.3	$2,050	-
DG-800 S 1:3[39]	CARF-Models (Dreamworks RC)	236	92	2032*	39	16	41	62.4	7.2	$4,600	TUM[40]
114" Extra NG[41]	Extreme Flight	1114	109	2390	39	16	41	53.0	24.7	$2,500	-
RV-8 70cc G2[42]	Flex Innovations	100	90	2015	25	30	120	62.9	3.1	$1,500	-
OV-10 Bronco 20cc[43]	Hangar 9 (Horizon Hobby)	83.8	85	1,277	29	26	90	99.2	6.5	$1,500	-
OV-10 Bronco 30cc[44]	Hangar 9 (Horizon Hobby)	108	113	2,268	42	13	31	55.9	2.7	$2,500	This work
CubCrafters XCub 60cc[45]	Hangar 9 (Horizon Hobby)	116	82	1908	31	24	77	66.4	4.0	$1,110	-
120 in Turbo Bushmaster V2[46]	Legacy Aviation (Extreme Flight)	121	95	1615	26	29	112	78.5	5.9	$1,775	-
140 in Turbo Bushmaster[47]	Legacy Aviation (Extreme Flight)	138	108	2333	35	20	57	54.3	3.2	$2,625	-
Cessna 310[48]	RC Warbird Models	126	85	1990	35	20	57	63.7	4.0	$2,400	-
B-25 Mitchell 20cc[49]	Seagull Models (Legend Hobby)	95	76	1191	26	29	112	106.4	8.5	$2,400	-
Air Tractor AT-802A 50cc-60cc[50]	Seagull Models (Legend Hobby)	118	72.8	1,612	27.6	27.4	99	78.6	5.8	$1,350	-
Pilatus PC-21 XL V2[51]	SebArt	83	93	1395	20.9	34.1	163	90.8	5.4	$2,450	-
Giles G-202 2.5m[52]	SebArt	98	100	1327	28	27	96	95.5	7.1	$1,900	-
27% Cessna 182 V2[53]	TMMY Composite (Austars Model)	120	94.5	1700*	39.6	15.4	39	74.5	5.3	$3,700	-
150" DC-3[54]	TMMY Composite (Austars Model)	150	97	2454*	51	4	8	51.6	3.2	$4,200	-
A-10 EDF 1:7.75[55]	Skymaster Jet Models (Pacific RC Jets)	88.4	82	1213*	35.2	19.8	56	104.5	7.6	$3,200	-

Notes: * Designates approximate input data. Weights given are the upper bound of what the manufacturer provides. Costs are at time of writing (May 2026) and include estimated shipping costs to Indiana University, Bloomington, IN, USA.

(a) Bill Hempel 25% Piper J-3 Clipped Wing Cub (image from [56])

(b) Bill Hempel 25% Piper PA-25 Pawnee (image from [57])

(c) Bill Hempel 40% Piper J-3 Clipped Wing Cub (image from [37])

(d) Bill Hempel 40% Piper PA-18 Super Cub (image from [58])

(e) CARF-Models DG-800 S 1:3 (image from [59])

(f) Extreme Flight 114" Extra NG (image from [41])

(g) Flex Innovations RV-8 70cc (image from [42])

(h) Hangar 9 OV-10 Bronco 20cc (image from [43])

(i) Hangar 9 Cub Crafters Xcub 60cc (image from [45])

(j) Hangar 9 OV-10 Bronco 30cc (image from [44])

(k) Legacy Aviation 120 in Turbo Bushmaster V2 (image from [46])

(l) Legacy Aviation 140 in Turbo Bushmaster (image from [47])

(m) RC Warbird Models Cessna 310 (image from [48])

(n) Seagull Models B-25 20cc (image from [49])

(o) Seagull Models AT-802A 50cc-60cc (image from [50])

(p) SebArt Pilatus PC-21 XL V2 (image from [51])

(q) SebArt Giles G-202 2.5m (image from [52])

(r) TMMY 27% Cessna 182 V2 (image from [60])

(s) TMMY 150" DC-3 (image from [61])

(t) Skymaster A-10 EDF 1:7.75 (image from [55])

Figure 5. Photographs of the surveyed RC model aircraft, each shwon with a person in order to provide scale.

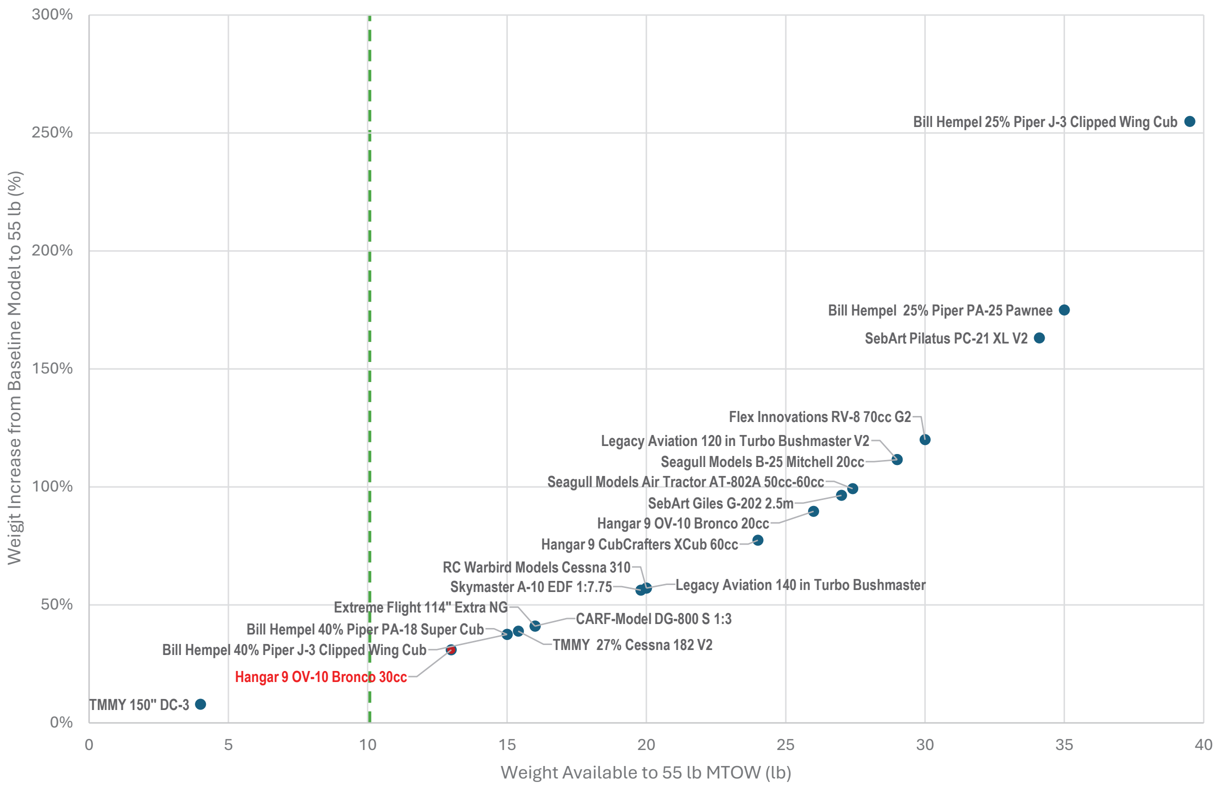

Figure 6. Plot of trade study data from identified potential UAVs. Weight is plotted on the x-axis and weight increase as a percentage is plotting on the y-axis.

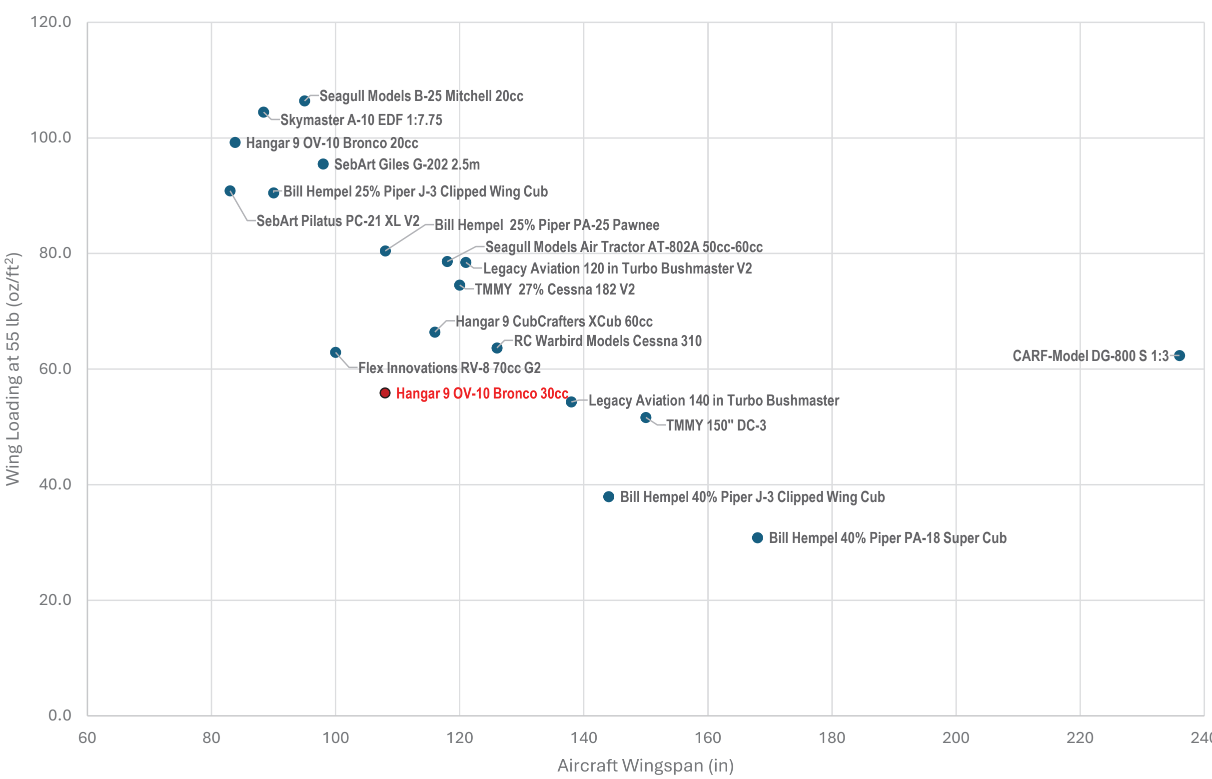

Figure 7. Plot of trade study data from identified potential UAVs. Wingspan is plotted on the x-axis and wing loading is plotted on the y-axis.

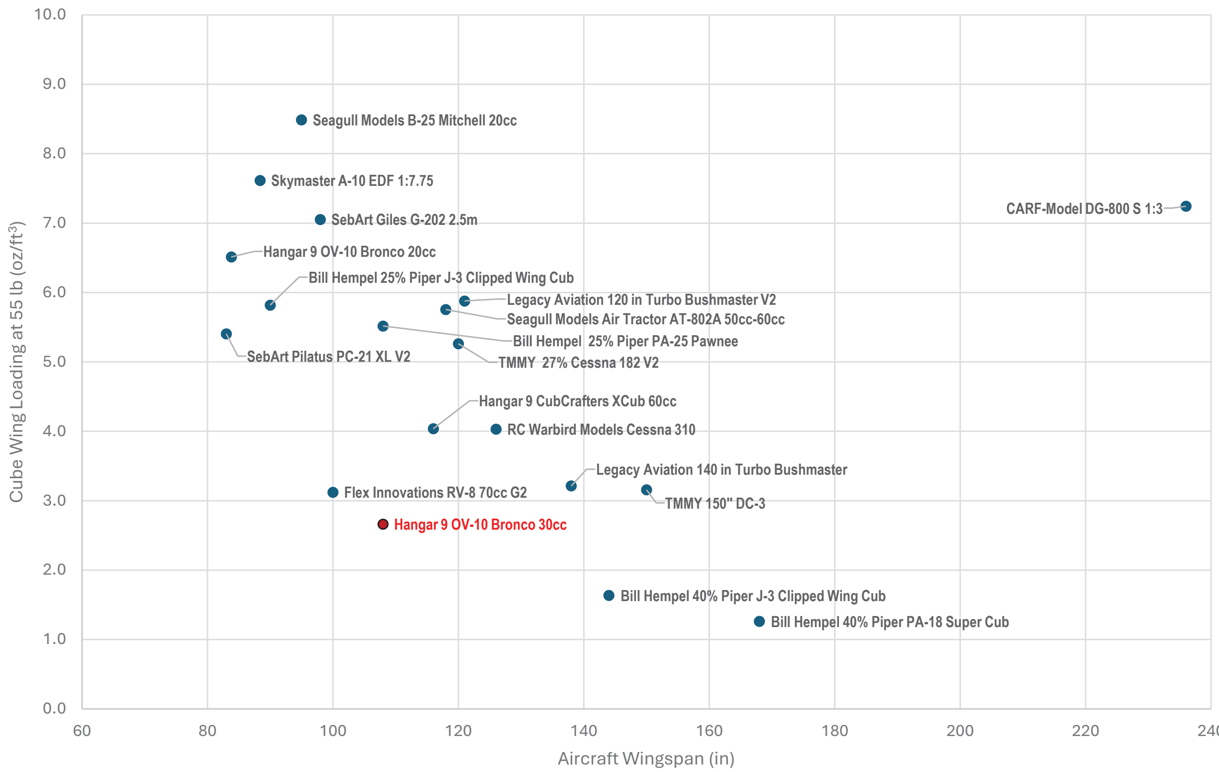

Figure 8. Plot of trade study data from identified potential UAVs. Wingspan is plotted on the x-axis and cubic wing loading is plotted on the y-axis.

V. Aircraft Development and Testing Plan

A. Aircraft Development

The Hangar 9 OV-10 Bronco 30cc ARF was selected as the development UAV testbed because it provided the payload capacity and internal volume required for integration of the planned data recording payload. The stock airframe, shown in Fig. 9, and the corresponding three-view drawing, shown in Fig. 10, illustrate the large fuselage and twin-engine layout available for payload mounting and system integration. Although the final flight-ready data acquisition hardware was expected to be more compact than the benchtop prototype, the larger airframe was selected to reduce integration risk and provide additional volume margin for future payloads and supporting instrumentation.

The key physical properties of the airframe are summarized in Table 3. These include the manufacturer-provided aircraft dimensions, baseline airframe weight, measured instrumentation weight, and estimated total gross weight with the payload installed. The aircraft component configuration used for the initial flight test is listed in Table 4, including the selected flight control hardware, receiver power system, electric propulsion components, and motor flight packs.

Several modifications were made to the stock aircraft to improve reliability for the planned payload-equipped configuration. Stronger control linkages were installed to improve the durability of the flap and aileron connection points. The pushrods, ball links, and servos for the flaps, ailerons, elevator, and rudders were also upgraded with higher-quality components to reduce the likelihood of control-system failure during flight. These modifications were motivated by the increased loads expected from future payload operation and by commonly reported failure modes for this class of scale RC aircraft.

Additional payload margin was created by omitting nonessential stock accessories during assembly. Components such as simulated exhaust ports and external mounting pylons were excluded because they were primarily cosmetic and were not required for the initial flight evaluation of the aircraft. In total, these changes reduced the aircraft mass by approximately 1.5 kg relative to the fully equipped stock configuration.

Figure 9. Completed Hangar 9 OV-10 Bronco 30cc testbed following the initial baseline flight, shown after successful recovery and post-flight inspection.

The initial electric propulsion configuration was selected to prioritize compatibility, reliability, and safe first-flight operation. Therefore, the E-Flite Power 180 motor and 12S 5000 mAh battery setup were selected based on manufacturer recommendations. A Castle Creations Phoenix Edge HV 120 ESC was used to accommodate the expected current draw. The manufacturer-recommended propeller options included the APC-E 20×10 and 18×12 Thin Electric; however, the initial configuration used APC-E 20×10 Thin Electric propellers. This baseline propulsion configuration was used for the first flight test before additional propulsion configurations or payload conditions were evaluated.

Alternative propulsion systems were identified during the development process but were not flight tested in this phase of the work. Candidate options included smaller and potentially more efficient Hacker A60-XS series motors, reduced-diameter APC-E 18×10 and 16×10 Thin Electric propellers, and lower-voltage 8S battery configurations. These combinations were estimated using manufacturer data and propulsion-analysis tools, including eCalc motor calculations. Evaluation of these alternative propulsion configurations was deferred to future work after additional airframe reliability improvements are completed.

A layout of the developed system is given in Fig. 11. The labels correspond to the components listed in Table 4 as it was used during the first flight test. Future versions of the aircraft layout will include a more complete discussion of component placement, center-of-gravity management, and the integration of the expected 4.3 kg instrumentation payload.

Table 3. Airframe physical specifications.

Geometric Properties	
Overall Length	113.0 in (2870 mm)
Wingspan	108.0 in (2743 mm)
Wing Area	2268 in^2 (146.3 dm^2)
Wing Aspect Ratio	5.14
Inertial Properties	
Manufacturer Airframe Weight Range	40-42 lb (18.1-19.1 kg)
Assembled Stock Configuration Weight	46.56 lb (21.12 kg)
Payload Integration Weight Budget	
Measured Instrumentation Weight	9.4 lb (4.28 kg)
Max Allowable Airframe Weight	45.5 lb (20.62 kg)
Total Gross Weight	54.9 lb (24.90 kg)
Necessary Weight Reduction	1.06 lb (0.48 kg)

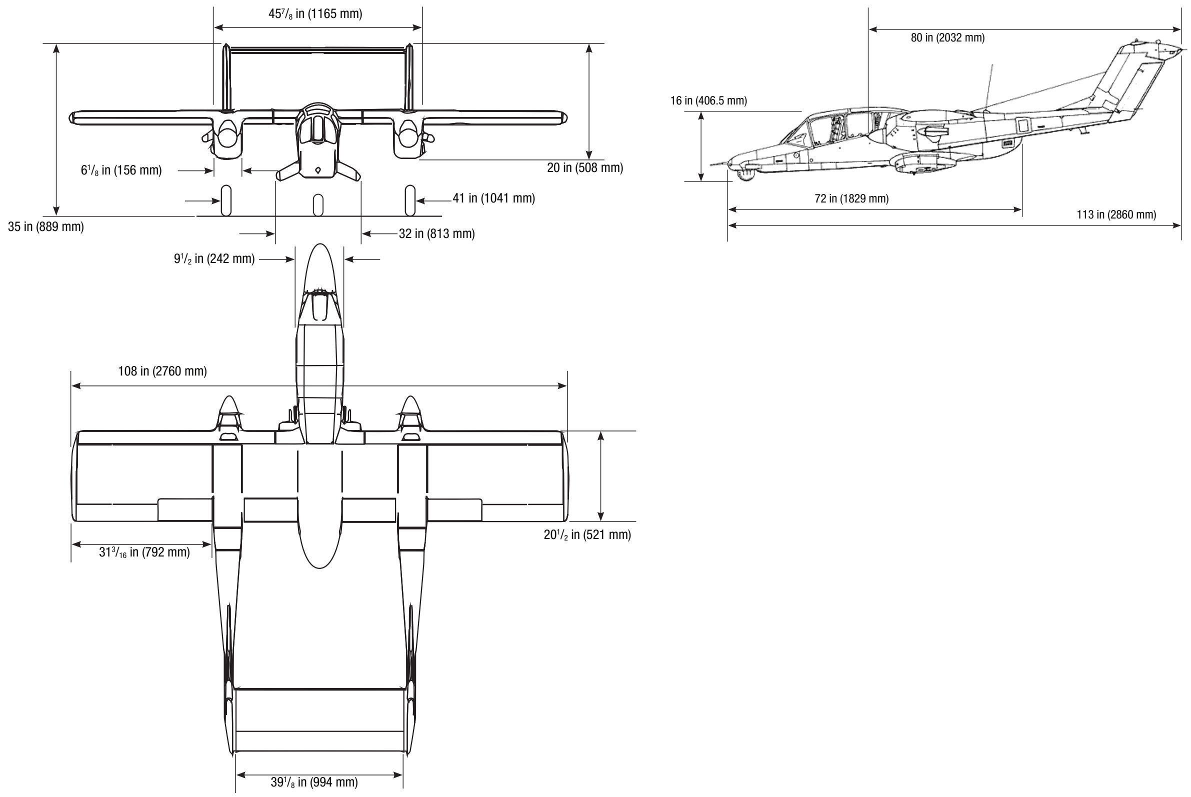

Figure 10. A 3-view of the Bronco UAV Testbed airframe (image adapted from the manufacturer manual)[62]

Table 4. Airframe component specifications for the current aircraft configuration.

Airframe	
Model	Hangar 9 OV-10 Bronco 30cc ARF, 108"
Construction	Built-up balsa and plywood structure, aluminum retractable landing gear, fiberglass cowl, and styrene canopy.
Flight Controls	
Control Surfaces	(2) Ailerons, elevator, (2) rudders, (4) flaps, nosewheel, and (2) throttle
Transmitter	Futaba T32MZ
Receiver	Futaba R7014HS
Servos	(4) Hitec HSB-9465SH, (5) Hitec HSB-9475SH, Hitec HSB-9380TH
Power Distribution	SmartFly PowerSystem Sport Plus
Receiver Battery	(2) Thunder Power ProLite 25c 2S 7.4V 2,200 mAh
Landing Gear Battery	(1) Thunder Power ProLite 25c 2S 7.4V 2,200 mAh
Propulsion	
Motor	E-Flite Power 180 Outrunner 195KV
ESC	Castle Creations Phoenix Edge HV 120
Propeller	(2) APC-E 20×10 Thin Electric
Motor Flight Pack	(4) Thunder Power Elite 55c 6S 22.2V 5000 mAh in series as 12S, one set per motor
Motor Power Switch	(2) Emcotec SPS 70V 60/120A

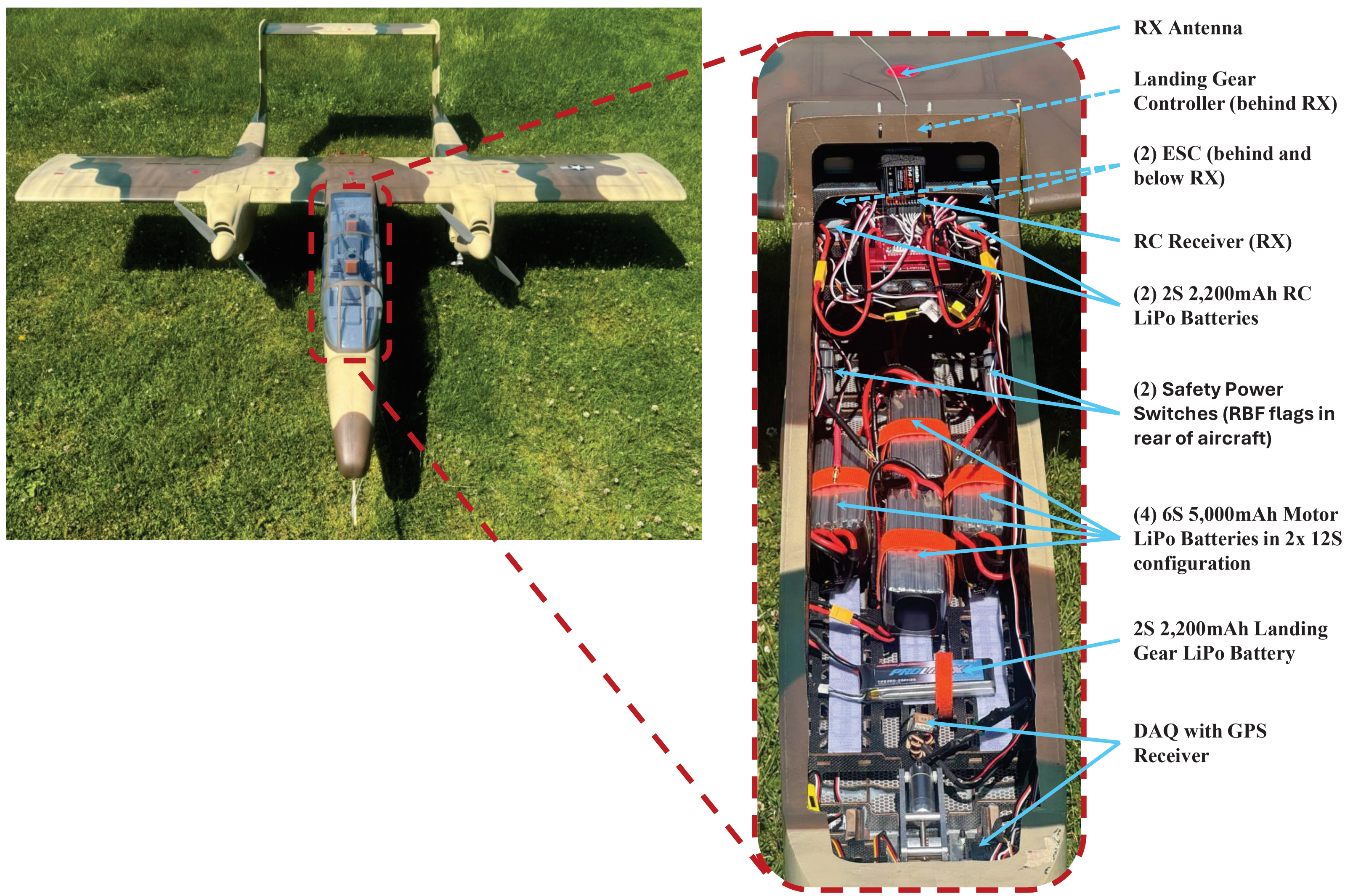

Figure 11. Labeled view of the developed Bronco testbed.

B. Flight Test Design and Instrumentation

The initial flight test was designed as a conservative shakedown flight of the stock-weight aircraft configuration. The objective was to verify basic aircraft assembly, control-surface effectiveness, propulsion-system operation, landing-gear function, and general handling qualities before testing higher-risk payload or propulsion configurations. Although a broader test matrix was originally developed to compare multiple motor, propeller, battery, and payload configurations, these additional configurations were not tested during this phase because the first flight resulted in a partial landing-gear failure after touchdown. As a result, the present work reports only the initial baseline flight test.

Three onboard data logging sources were included for the first flight. A legacy Eagle Tree Systems data acquisition system was installed to record GPS speed, airspeed, and four PWM channels corresponding to aileron, elevator, rudder, and throttle commands. In addition, each Castle Creations ESC recorded propulsion data for its corresponding motor, including motor RPM, throttle PWM, voltage, current, and electrical power. These systems were intended for post-flight review and did not transmit data to the ground during flight. Although all logging systems were tested before the flight day, the Eagle Tree data acquisition system did not record during the first flight. Therefore, only the ESC-based propulsion data is presented for the initial flight-test discussion.

Prior to flight, a radio range test was conducted to verify control-system performance. The aircraft was first tested with only the radio-control system powered, and control authority was verified at a range of approximately 4000 ft. This distance exceeded the expected line-of-sight operating range of approximately 1500–2000 ft for the planned flight. The controls were then checked with all aircraft systems powered, including the landing gear and propulsion system. The propulsion system was ground run to approximately 60–75% throttle while verifying proper control response at close range and at approximately 400 ft, corresponding to the approximate runway length used for the test. All systems functioned as expected during these preflight checks.

VI. Flight Testing

The first flight test was conducted to evaluate the baseline stock-weight aircraft configuration prior to payload integration. The test was intended to minimize aircraft risk while verifying takeoff behavior, climb performance, control response, flap operation, cruise handling, and landing behavior. Weather during the flight was sunny, with an ambient temperature of approximately 77°F (25°C). Winds were variable in direction at approximately 6-9 mph, with gusts up to 13 mph.

For takeoff, the aircraft was configured with takeoff flaps set to approximately 30° and aligned down the runway toward the dominant wind direction. Although the wind direction was variable, the takeoff direction was selected to provide the most favorable headwind component available at the time. Throttle was applied gradually, and the aircraft accelerated down the runway. Rotation occurred at approximately 50-60% throttle. The pilot maintained slight up-elevator during the takeoff roll, and the aircraft lifted off once it reached flying speed rather than through an abrupt rotation command.

After liftoff, the pilot allowed the aircraft to climb gradually before increasing throttle to approximately 64% near the end of the runway. The aircraft then entered a higher-angle climb and turned into a racetrack pattern. During this initial climb, the maximum observed electrical power was approximately 3.6 kW per motor as seen in Fig. 12. This exceeded the nominal 3.0 kW maximum motor power specification, despite the propulsion-system configuration being based on manufacturer-recommended components. This observation indicated that additional propulsion characterization is needed before future higher-weight or extended-duration operation.

The aircraft was flown through multiple racetrack patterns during the flight. The first portion of the flight was conducted with the flaps still in the takeoff configuration, after which the flaps were fully retracted. The flaps were later lowered again to the takeoff position for an additional racetrack pattern before landing. Throughout the flight, the aircraft demonstrated stable basic handling and controllability in the baseline configuration. The major aircraft subsystems, including the twin electric propulsion system, flight controls, flap system, and radio-control system, were successfully demonstrated in flight.

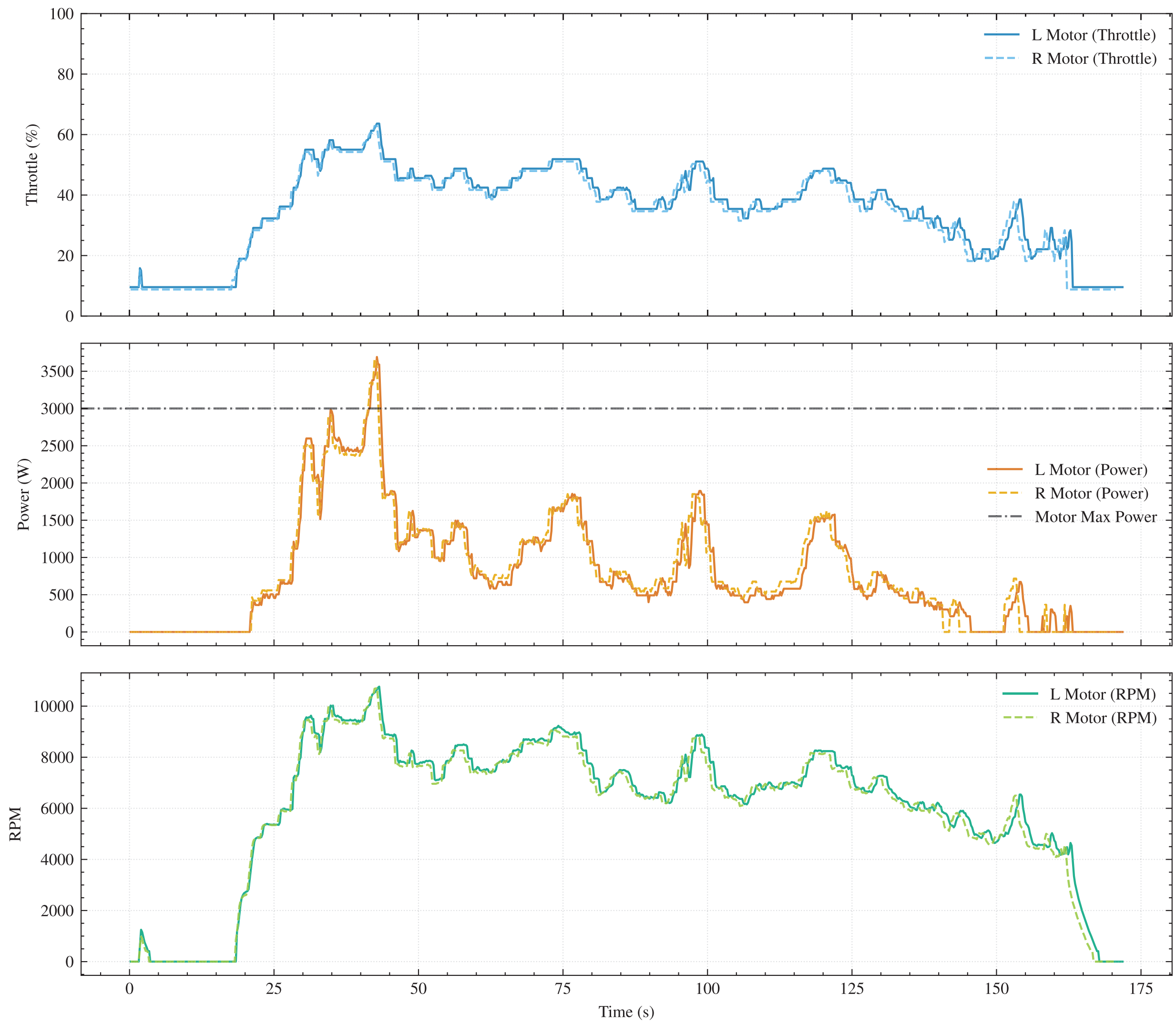

Figure 12. Motor performance data recorded by the left and right ESCs during the initial baseline flight test.

During landing, the pilot flew a long approach into the dominant wind direction. A slight crosswind was present, and the aircraft crabbed approximately 10-20° left of the runway centerline during the approach. Near the ground, the aircraft was flared with slight throttle added to reduce descent rate. The aircraft touched down on the runway centerline in a nose-up attitude, with the right main landing gear contacting slightly before the left main landing gear as can be seen in Fig. 13(b) and Fig. 13(c). After the aircraft had substantially decelerated and while the pilot was correcting the rollout toward the centerline, the aircraft drifted slightly left. At low speed, the left wheel separated from the axle after the retaining C-clip detached. The aircraft then veered left off the runway into the adjacent cut grass area.

The landing-gear issue did not cause additional damage to the airframe; however, spare hardware was not available at the field, so no additional flights were conducted that day. The aircraft was returned to the development lab for repair and inspection. Landing-gear retention and durability issues are known concerns for this aircraft based on prior hobbyist reports, but the occurrence of this issue on the first flight was unexpected. As a result, additional configuration testing, payload testing, and propulsion comparisons were deferred until the landing gear could be improved and the aircraft could be returned to a reliable test condition.

Overall, the first flight was considered a successful baseline demonstration of the aircraft and its major subsystems. The aircraft completed takeoff seen in Fig. 13(a), climb, racetrack-pattern flight, flap deployment and retraction,

(a) (b) (c)

Figure 13. Initial baseline flight sequence of the Hangar 9 OV-10 Bronco 30cc UAV testbed, showing the aircraft during takeoff in (a) and during landing in (b) and (c).

approach, and touchdown. However, the partial landing-gear failure prevented further testing during the same flight day and highlighted the need for additional reliability improvements before expanding the flight envelope or integrating the full payload. Future flight tests will focus on improving landing-gear robustness, repeating baseline performance measurements with reliable data logging, and then evaluating payload and propulsion configurations after the aircraft reliability issues have been addressed.

VII. Summary

This work introduced the preliminary development of a large fixed-wing UAS testbed for future event-camera-based aviation research. The motivation for the platform was driven by the need for fixed-wing flight data that better represents long-endurance aircraft operation for future event-camera datasets. To support this goal, a new multimodal sensor payload was defined that includes stereo event cameras, synchronized global-shutter frame cameras, inertial sensing, onboard computation, data acquisition hardware, and an independent payload power system.

A bench top implementation of the sensor suite was used to estimate the mass, compute, power, and integration requirements of the future payload. This preliminary system characterization indicated that the aircraft must support an instrumentation payload of approximately 4.28 kg while also providing sufficient internal volume for mounting hardware, cable routing, power distribution, and future vibration isolation. These requirements were then used to guide the aircraft selection process.

A survey of commercially available large-scale RC aircraft was conducted to identify platforms capable of supporting the required payload while remaining below the 55 lb operational weight constraint. Candidate aircraft were compared based on size, payload margin, configuration, internal volume, cost, and suitability for future sensing applications. The Hangar 9 OV-10 Bronco 30cc ARF was selected as the development testbed due to its twin-engine configuration, large fuselage volume, payload capacity, and suitability for centrally mounted sensing hardware. The twin-engine configuration also provides an opportunity to reduce propeller-induced sensing interference compared with the previous wing-boom-mounted sensor configuration from prior work.[25]

The aircraft was modified to improve reliability and payload-carrying capability. These modifications included upgraded control linkages, improved control hardware, higher-quality servos for key control surfaces, and removal of nonessential cosmetic components to reduce aircraft mass. The initial aircraft configuration used the stock recommended electric propulsion architecture and was flown without the surrogate payload to reduce first-flight risk.

The first flight test demonstrated the baseline aircraft configuration and verified operation of the major flight systems. The aircraft successfully completed takeoff, climb, racetrack-pattern flight, flap operation, approach, and touchdown. ESC-based propulsion logs were recorded, although the Eagle Tree data acquisition system did not record during the flight. The propulsion data indicated a peak electrical power of approximately 3.6 kW per motor during the initial climb, which exceeded the nominal motor maximum power specification and motivates further propulsion characterization.

The initial flight also revealed a landing-gear reliability issue when the left wheel separated from the axle after touchdown due to loss of the retaining C-clip. Although no major airframe damage occurred, the issue prevented further flights that day and delayed the planned evaluation of additional payload and propulsion configurations. Therefore, the present work should be viewed as the first stage of Bronco UAS development: aircraft selection, baseline assembly, preliminary flight validation, and identification of key reliability improvements required before full payload testing.

VIII. Future Work

Future work will first focus on improving the reliability of the landing gear before expanding the flight-test envelope. The initial flight showed that the aircraft could complete the planned baseline flight profile, but the wheel-retention failure after touchdown indicated that the stock landing-gear hardware requires additional attention before repeated research flights can be conducted. Planned improvements include inspection of the wheel-retention design, replacement or reinforcement of retaining hardware, and additional ground-roll testing prior to subsequent flights.

After the landing gear is improved, baseline flight testing will be repeated with verified operation of all onboard data logging systems. In particular, the Eagle Tree data acquisition system will be repaired, replaced, or reconfigured to ensure reliable recording of GPS speed, airspeed, and control PWM channels. These measurements will be combined with the ESC propulsion logs to support quantitative analysis of aircraft speed, throttle setting, motor RPM, voltage, current, and electrical power during future flights.

The broader propulsion and payload test matrix originally planned for this work will be completed in future testing. These flights will compare the stock propulsion configuration against candidate lower-weight and potentially more efficient propulsion systems. Candidate configurations include Hacker A60-XS series motors, smaller APC-E 18×10 and 16×10 Thin Electric propellers, smaller ESCs, and 6S-8S battery configurations. These options will be evaluated to determine whether propulsion-system weight and electrical power consumption can be reduced while maintaining acceptable takeoff, climb, cruise, and landing performance.

Future work will also include flight testing with a surrogate payload representing the planned 4.28 kg instrumentation package. These tests will be used to evaluate the aircraft near the 55 lb maximum takeoff weight limit while avoiding risk to the full sensor payload during early testing. Particular attention will be given to center-of-gravity placement, payload mounting, battery distribution, and the effect of added mass on takeoff distance, climb performance, cruise throttle setting, low-speed handling, and landing behavior. The aircraft component layout will be refined based on these results to better distribute mass and preserve adequate payload margin for batteries and instrumentation.

The next major phase of development will integrate the full multimodal data collection payload into the aircraft. This payload will include event cameras, frame cameras, onboard computation, data acquisition hardware, power electronics, and vibration isolation hardware. Ground testing will be performed before flight to verify synchronization, data bandwidth, storage reliability, payload power performance, and thermal behavior.

After payload integration, flight testing will be expanded to collect synchronized event-camera, frame-camera, inertial, airspeed, GPS, propulsion, and aircraft-state data. These flights will be used to evaluate the quality of the recorded sensor data under realistic fixed-wing flight conditions, including changes in speed, altitude, lighting, aircraft attitude, and background clutter. The resulting data will support future development of event-based perception algorithms to enable fixed-wing autonomy.

A further goal of this platform is the integration of an autonomous software stack for repeatable trajectory execution. Planned autonomy capabilities include waypoint navigation, spline-based path following, and eventually closed-loop evaluation of perception-informed guidance algorithms. Repeatable autonomous flight paths will improve the consistency of future dataset collection and allow sensor and algorithm performance to be compared across controlled flight conditions.

This work represents the first stage of a broader Bronco UAS development effort. The follow-on study will focus on landing-gear reliability improvements, expanded baseline flight testing, propulsion and payload configuration evaluation, full sensor-payload integration, and initial dataset generation using the selected aircraft platform.

IX. Acknowledgments

This work was made possible through funding provided to the first author by the NSWC Crane Naval Innovation Science & Engineering (NISE) Program, the ONR Independent Applied Research (IAR) Program, and the DoW Science Mathematics and Research for Transformation (SMART) Scholarship-for-Service Program.

References

[1]Gehrig, D. and Scaramuzza, D., "Low-latency automotive vision with event cameras," *Nature*, Vol. 629, No. 8014, 2024, pp. 1034–1040.

[2]Maqueda, A. I., Loquercio, A., Gallego, G., García, N., and Scaramuzza, D., "Event-Based Vision Meets Deep Learning on Steering Prediction for Self-Driving Cars," *2018 IEEE/CVF Conference on Computer Vision and Pattern Recognition*, June 2018, pp. 5419–5427, ISSN: 2575-7075.

[3]Bonazzi, P., Vogt, C., Jost, M., Khacef, L., Paredes-Vallés, F., and Magno, M., "Towards Low-Latency Event-based Obstacle Avoidance on a FPGA-Drone," May 2025, arXiv:2504.10400 [cs].

[4]Dimitrova, R. S., Gehrig, M., Brescianini, D., and Scaramuzza, D., "Towards Low-Latency High-Bandwidth Control of Quadrotors using Event Cameras," *2020 IEEE International Conference on Robotics and Automation (ICRA)*, May 2020, pp. 4294–4300, ISSN: 2577-087X.

[5]Vitale, A., Renner, A., Nauer, C., Scaramuzza, D., and Sandamirskaya, Y., "Event-driven Vision and Control for UAVs on a Neuromorphic Chip," *2021 IEEE International Conference on Robotics and Automation (ICRA)*, May 2021, pp. 103–109, ISSN: 2577-087X.

[6]Bauersfeld, L. and Scaramuzza, D., "Low-Latency Event-Based Velocimetry for Quadrotor Control in a Narrow Pipe," July 2025, arXiv:2507.15444 [cs].

[7]Messikommer, N., Fang, C., Gehrig, M., Cioffi, G., and Scaramuzza, D., "Data-Driven Feature Tracking for Event Cameras With and Without Frames," *IEEE Transactions on Pattern Analysis and Machine Intelligence*, Vol. 47, No. 5, 2025, pp. 3706–3717.

[8]Wang, X., Wang, S., Tang, C., Zhu, L., Jiang, B., Tian, Y., and Tang, J., "Event Stream-Based Visual Object Tracking: A High-Resolution Benchmark Dataset and A Novel Baseline," *2024 IEEE/CVF Conference on Computer Vision and Pattern Recognition (CVPR)*, 2024, pp. 19248–19257.

[9]Sanket, N., Singh, C., Parameshwara, C. M., Fermüller, C., Croon, G., and Aloimonos, Y., "EVPropNet: Detecting Drones By Finding Propellers For Mid-Air Landing And Following," *Robotics: Science and Systems (RSS)*, 07 2021.

[10]Mitrokhin, A., Fermüller, C., Parameshwara, C., and Aloimonos, Y., "Event-Based Moving Object Detection and Tracking," *2018 IEEE/RSJ International Conference on Intelligent Robots and Systems (IROS)*, 2018, pp. 1–9.

[11]Zhao, C., Li, Y., and Lyu, Y., "Event-based Real-time Moving Object Detection Based On IMU Ego-motion Compensation," *2023 IEEE International Conference on Robotics and Automation (ICRA)*, 2023, pp. 690–696.

[12]Wang, X., Li, J., Zhu, L., Zhang, Z., Chen, Z., Li, X., Wang, Y., Tian, Y., and Wu, F., "VisEvent: Reliable Object Tracking via Collaboration of Frame and Event Flows," *IEEE Transactions on Cybernetics*, Vol. 54, No. 3, 2024, pp. 1997–2010.

[13]Monforte, M., Gava, L., Iacono, M., Glover, A., and Bartolozzi, C., "Fast Trajectory End-Point Prediction with Event Cameras for Reactive Robot Control," *2023 IEEE/CVF Conference on Computer Vision and Pattern Recognition Workshops (CVPRW)*, 2023, pp. 4036–4044.

[14]Zhang, J., Dong, B., Zhang, H., Ding, J., Heide, F., Yin, B., and Yang, X., "Spiking Transformers for Event-based Single Object Tracking," *2022 IEEE/CVF Conference on Computer Vision and Pattern Recognition (CVPR)*, 2022, pp. 8791–8800.

[15]Parameshwara, C. M., Sanket, N. J., Singh, C. D., Fermüller, C., and Aloimonos, Y., "0-MMS: Zero-Shot Multi-Motion Segmentation With A Monocular Event Camera," *2021 IEEE International Conference on Robotics and Automation (ICRA)*, 2021, pp. 9594–9600.

[16]Mitrokhin, A., Fermüller, C., Parameshwara, C., and Aloimonos, Y., "Event-Based Moving Object Detection and Tracking," *2018 IEEE/RSJ International Conference on Intelligent Robots and Systems (IROS)*, 2018, pp. 1–9.

[17]Sironi, A., Brambilla, M., Bourdis, N., Lagorce, X., and Benosman, R., "HATS: Histograms of Averaged Time Surfaces for Robust Event-based Object Classification," 2018.

[18]Orchard, G., Meyer, C., Etienne-Cummings, R., Posch, C., Thakor, N., and Benosman, R., "HFirst: A Temporal Approach to Object Recognition," *IEEE Transactions on Pattern Analysis and Machine Intelligence*, Vol. 37, No. 10, Oct. 2015, pp. 2028–2040.

[19]Lagorce, X., Orchard, G., Galluppi, F., Shi, B. E., and Benosman, R. B., "HOTS: A Hierarchy of Event-Based Time-Surfaces for Pattern Recognition," *IEEE Transactions on Pattern Analysis and Machine Intelligence*, Vol. 39, No. 7, 2017, pp. 1346–1359.

[20]Rodríguez-Gomez, J., Eguíluz, A. G., Martínez-de Dios, J., and Ollero, A., "Asynchronous event-based clustering and tracking for intrusion monitoring in UAS," *2020 IEEE International Conference on Robotics and Automation (ICRA)*, 2020, pp. 8518–8524.

[21]Pérez-Cutiño, M., Eguíluz, A. G., Dios, J. M.-d., and Ollero, A., "Event-based human intrusion detection in UAS using Deep Learning," *2021 International Conference on Unmanned Aircraft Systems (ICUAS)*, 2021, pp. 91–100.

[22]Alberico, I., Cannici, M., Cioffi, G., and Scaramuzza, D., "Egocentric Event-Based Vision for Ping Pong Ball Trajectory Prediction," 2025.

[23]Zhang, J., Dong, B., Zhang, H., Ding, J., Heide, F., Yin, B., and Yang, X., "Spiking Transformers for Event-based Single Object Tracking," *2022 IEEE/CVF Conference on Computer Vision and Pattern Recognition (CVPR)*, 2022, pp. 8791–8800.

[24]Sanket, N. J., Parameshwara, C. M., Singh, C. D., Kuruttukulam, A. V., Fermüller, C., Scaramuzza, D., and Aloimonos, Y., "EVDodgeNet: Deep Dynamic Obstacle Dodging with Event Cameras," *2020 IEEE International Conference on Robotics and Automation (ICRA)*, 2020, pp. 10651–10657.

[25]Coen, P., Cox, B., and Dantsker, O. D., "Development of a Fixed-Wing UAV Testbed for In-Flight Data Collection from an Event-Based Camera," Accepted to AIAA SciTech Forum 2026, Orlando, Florida.

[26]Zhu, A. Z., Thakur, D., Özaslan, T., Pfrommer, B., Kumar, V., and Daniilidis, K., "The Multivehicle Stereo Event Camera Dataset: An Event Camera Dataset for 3D Perception," *IEEE Robotics and Automation Letters*, Vol. 3, No. 3, 2018, pp. 2032–2039.

[27]Gehrig, M., Aarents, W., Gehrig, D., and Scaramuzza, D., "DSEC: A Stereo Event Camera Dataset for Driving Scenarios," *IEEE Robotics and Automation Letters*, 2021.

[28]Luxonis, "OAK-FFC AR0234 M12," https://shop.luxonis.com/products/oak-ffc-ar0234-m12, 2025.

[29]Luxonis, "OAK-FFC OV9282," https://shop.luxonis.com/products/oak-ffc-ov9282, 2025.

[30]Luxonis, “OAK-FFC AR0234 M12,” https://shop.luxonis.com/products/oak-ffc-4p, 2025.

[31]Rebecq, H., Ranftl, R., Koltun, V., and Scaramuzza, D., “High Speed and High Dynamic Range Video with an Event Camera,” *IEEE Transactions on Pattern Analysis and Machine Intelligence*, Vol. 43, No. 6, 2021, pp. 1964–1980.

[32]“U.S. Code Title 49 - Transportation,” .

[33]National Aeronautics and Space Administration, “MicroCub First Flight a Success,” NASA Website, 2018, Accessed: 2026-05-06.

[34]Dantsker, O., Mancuso, R., Ward, B., Miller, C., Shea, D., and Collins, K., “Flight Testing Instrumentation Development and Integration for a Subscale Integrated High Lift Propulsor Testbed,” *AIAA SciTech Forum*, No. 2416, 2025, AIAA Paper 2025-2416, AIAA SciTech Forum 2025, Orlando, FL.

[35]Bill Hempel, “30cc–50cc Clipped Wing Cub,” https://www.billhempel.com/cub/newcub25/index.html, Accessed May 2026.

[36]Bill Hempel, “25% Piper PA-25 Pawnee,” https://www.billhempel.com/pawnee/index.php, Accessed May 2026.

[37]Bill Hempel, “40% Clipped Wing Cub,” https://www.billhempel.com/CWC/40ClippedWingCub/index.php, Accessed May 2026.

[38]Bill Hempel, “40% Super Cub,” https://www.billhempel.com/supercub40/index.php, Accessed May 2026.

[39]CARF-Models, “DG-800 S 1:3, 6.0 m,” https://carf-models.com/en/products/dg-800-s, Accessed May 2026.

[40]Teubl, D., Sissing, T. B., and Hornung, M., “RETROFITTING A JET DRIVEN UAV TO FORM A MULTI-PURPOSE TEST PLATFORM,” *International Council of the Aeronautical Sciences*, 2024.

[41]Extreme Flight, “EF - 114” Extra NG,” https://extremeflightrc.com/collections/114-125/products/114-extra-ng-blue-white-silver, Accessed May 2026.

[42]Flex Innovations, “RV-8 70cc G1/G2 FLS,” https://flexinnovations.com/product/rv8-70cc-g2/, Accessed May 2026.

[43]Horizon Hobby, “Hangar 9 OV-10 Bronco 20cc ARF with Landing Gear Set,” https://www.horizonhobby.com/product/ov-10-bronco-20cc-arf-84”-with-landing-gear-set/HAN5055.html, Accessed May 2026.

[44]Horizon Hobby, “Hangar 9 OV-10 Bronco 30cc ARF, 108 in,” https://www.horizonhobby.com/product/ov-10-bronco-30cc-arf-108/HAN4670.html, Accessed May 2026.

[45]Horizon Hobby, “Hangar 9 CubCrafters XCub 60cc ARF,” https://www.horizonhobby.com/product/cubcrafters-xcub-60cc-arf/HAN5260B.html, Accessed May 2026.

[46]Extreme Flight, “Legacy 120 in Turbo Bushmaster V2 - Camouflage,” https://extremeflightrc.com/collections/bushmaster-arfs/products/120-turbo-bushmaster-v2-red-black-copy, Accessed May 2026.

[47]Extreme Flight, “Legacy 140 in Turbo Bushmaster - Camouflage,” https://extremeflightrc.com/collections/bushmaster-arfs/products/140-turbo-bushmaster-camouflage, Accessed May 2026.

[48]RC Warbird Models, “126 in Cessna 310,” https://rcwarbirdmodels.com/products/126-cessna-310, Accessed May 2026.

[49]Gator-RC, “Seagull Models Mitchell B-25 20cc ARF - 95 in Wingspan,” https://www.gator-rc.com/products/seagull-models-mitchell-b-25-20cc-arf-95-inch, Accessed May 2026.

[50]Legend Hobby, “Air Tractor AT-802A 50cc-60cc ARF,” https://www.legendhobby.com/products/air-tractor-at-802a-118-60cc-arf-legend-hobby, Accessed May 2026.

[51]SebArt, “Pilatus PC-21 XL V2,” https://www.sebart.it/IMAC%2050-60cc.html, Accessed May 2026.

[52]SebArt, “Giles G-202 2.5m IMAC Pro,” https://www.sebart.it/IMAC%20100-120cc.html, Accessed May 2026.

[53]Austars Model, “120 Inch Composite Cessna-182 New Version V2,” https://www.austars-model.com/120-inch-composite-cessna182-new-version-v2-customized-paint-for-pre-order-2025-version_g122.html?s_id=5, Accessed May 2026.

[54]Austars Model, “150 Inch Composite DC-3 New Version 2025 with Optional Cowl Upgraded,” https://www.austars-model.com/150-inch-composite-dc3-new-version-2025-with-optional-cowl-upgraded_g2470.html?s_id=5, Accessed May 2026.

[55]Skymaster Jet Models, “A-10 EDF 1:7.75,” http://www.skymasterjets.net/ea10.htm, Accessed May 2026.

[56]FlyingGiants, “Thread Gallery,” https://www.flyinggiants.com/forums/thumbgallery.php?t=86497do=threadgallery, Accessed May 2026.

[57]YouTube, “Bill Hempel Piper Pawnee 25% RC Airplane Vol.7,” https://www.youtube.com/watch?v=7QGRa2WOV8g, Accessed May 2026.

[58]YouTube, “40% Scale Bill Hempel Super Cub - DLE 111cc Flat Twin Petrol - Jack at NLMFC Baldock #1 - 2022,” https://www.youtube.com/watch?v=3_vdQcSw890, Accessed May 2026.

[59]YouTube, “DG-800 S 1:3 CARF MODELS — 6m scale jet turbine RC glider — 4K — 2023,” https://www.youtube.com/watch?v=71PjM8UgW7I, Accessed May 2026.

[60]YouTube, “TMMY 1/5 Scale Cessna - Terrible Maiden Flight,” https://www.youtube.com/watch?v=$_xg7X2zSlx8, AccessedMay$2026.

[61]YouTube, “Ians150 Inch Austars DC3 Taxi test,” https://www.youtube.com/watch?v=VMzCDIOjql0, Accessed May 2026.

[62]Hobby, H., “Hangar 9 OV-10 Bronco 30cc, Instruction Manual,” https://www.horizonhobby.com/on/demandware.static/-/Sites-horizon-master/default/dw81b16650/Manuals/HAN4670-Manual-MULTI.pdf, 2025.